AD-A037 405 ENVIRONMENTAL RESEARCH AND TECHNOLOGY INC CONCORD MASS F/G 17/5
AN ALGORITHM TO RETRIEVE WATER VAPOR INFORMATION FROM SATELLITE--ETC(U)
NOV 76 R K CRANE N00228-75-C-2378

UNCLASSIFIED NEPRF-TR 7-76 (ERT) NL

1 OF 1
AD A037405

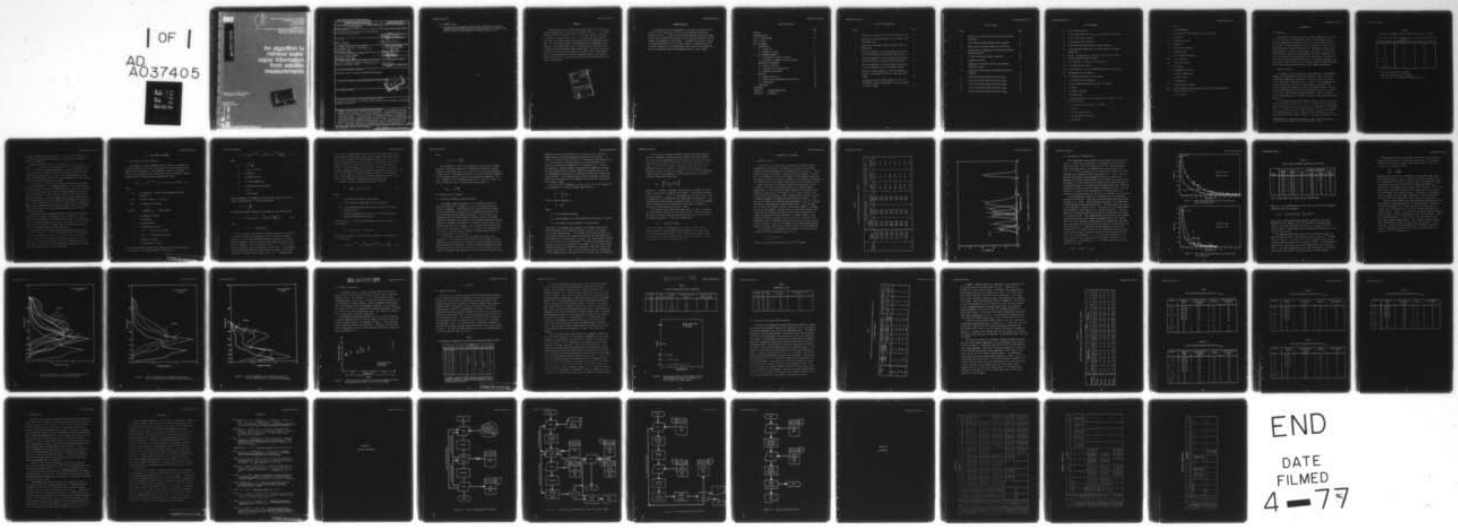

END
DATE FILMED
4-77

ERT

NEPRF Technical Report 7-76(ERT)
Document No. P-1423
Final Report
November 1976

Prepared for
Naval Environmental Prediction Research Facility
Naval Postgraduate School
Monterey, California 93940

An algorithm to retrieve water vapor information from satellite measurements

Prepared by
Robert K. Crane

ENVIRONMENTAL RESEARCH & TECHNOLOGY, INC.
CONCORD, MASS. • CHICAGO • LOS ANGELES • WASHINGTON, D.C.

SECURITY CLASSIFICATION OF THIS PAGE (When Data Entered)

REPORT DOCUMENTATION PAGE		READ INSTRUCTIONS BEFORE COMPLETING FORM
1. REPORT NUMBER NAVENVPREDRSCHFAC Technical Report 7-76 (ERT)	2. GOVT ACCESSION NO.	3. RECIPIENT'S CATALOG NUMBER
4. TITLE (and Subtitle) An Algorithm to Retrieve Water Vapor Information from Satellite Measurements		5. TYPE OF REPORT & PERIOD COVERED Final
		6. PERFORMING ORG. REPORT NUMBER NEPRF TR 7-76 (ERT)
7. AUTHOR(s) Robert K. Crane		8. CONTRACT OR GRANT NUMBER(s) N00 228-75-C-2378
9. PERFORMING ORGANIZATION NAME AND ADDRESS Environmental Research & Technology, Inc. 696 Virginia Road Concord, MA 01742		10. PROGRAM ELEMENT, PROJECT, TASK AREA & WORK UNIT NUMBERS Air Task A370370C/076C/ SW3713000 NEPRF WU 055: 3-5
11. CONTROLLING OFFICE NAME AND ADDRESS Naval Air Systems Command Department of the Navy Washington, D.C. 20361		12. REPORT DATE November 22, 1976
		13. NUMBER OF PAGES 37
14. MONITORING AGENCY NAME & ADDRESS (if different from Controlling Office) Naval Environmental Prediction Research Facility Monterey, California 93940		15. SECURITY CLASS. (of this report) Unclassified
		15a. DECLASSIFICATION/DOWNGRADING SCHEDULE

16. DISTRIBUTION STATEMENT (of this Report)

Approved for public release; distribution unlimited.

17. DISTRIBUTION STATEMENT (of the abstract entered in Block 20, if different from Report)

18. SUPPLEMENTARY NOTES

19. KEY WORDS (Continue on reverse side if necessary and identify by block number)

infrared remote sensing, water vapor, water vapor profile retrievals, statistical parameter estimation

20. ABSTRACT (Continue on reverse side if necessary and identify by block number)

Radiance values for the eight water vapor channels on the DMSP/SSH infrared sounder were simulated for cloud free conditions. The simulated values were inverted using a statistical multiple regression procedure to estimate total precipitable water. Inversions were also obtained using both the infrared water vapor channel data and temperature profile data. For the sounder channels incorporated into the DMSP/SSH sensor package, profile measurements are not possible below the height of the tropopause using the infrared channel data alone. Successful inversions with more than an 80 percent reduction of

20. ABSTRACT (cont)

variance from climatological values were accomplished using both temperature profile data (perhaps obtained from the CO_2 channel data) and one or more infrared water vapor channel observations.

ABSTRACT

Radiance values for the eight water vapor channels on the DMSP/SSH infrared sounder were simulated for cloud free conditions. The simulated values were inverted using a statistical multiple regression procedure to estimate total precipitable water. Inversions were also obtained using both the infrared water vapor channel data and temperature profile data. For the sounder channels incorporated into the DMSP/SSH sensor package, profile measurements are not possible below the height of the tropopause using the infrared channel data alone. Successful inversions with more than an 80 percent reduction of variance from climatological values were accomplished using both temperature profile data (perhaps obtained from the CO_2 channel data) and one or more infrared water vapor channel observations.

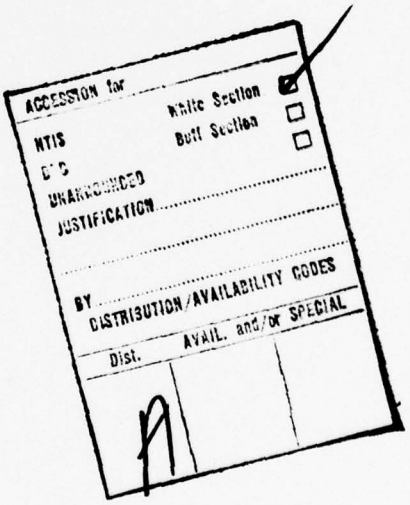

ACKNOWLEDGEMENTS

The author wishes to acknowledge the assistance provided for this project by Mr. Roland Nagle at the Naval Environmental Prediction Research Facility. He also wishes to acknowledge the work of Mr. Roger Weichel who developed the algorithm for the continuum correction and the computer programming for this project. In addition, he wishes to thank Dr. Robert McClatchey of the Air Force Geophysics Laboratory who provided the absorption line transmittance values used in the program and Mr. David Chang who directed the program during its early stages.

TABLE OF CONTENTS

LIST OF ILLUSTRATIONS

LIST OF TABLES

LIST OF SYMBOLS

B_ν is the Planck radiance

$\underline{C}$ is the correlation matrix with C_{ij} an element of the matrix

c_1 is the first Planck constant

c_2 is the second Planck constant

C_s is the continuum coefficient for self broadening

C_n is the continuum coefficient for total pressure (nitrogen) broadening

C_i are the contributions by lines at ν_i with the line width pressure dependence made explicit

d_j is an element of a data set or data vector

$\underline{d}^1$ is a modified data vector

$\underline{\underline{D}}$ is the D matrix, a set of coefficients used to relate $\underline{d}$ to $\underline{v}$

D_{ij} are elements of the D matrix

e is the partial pressure of water vapor

g is acceleration due to gravity

g_i is the transmission function for the i^{th} channel

H is height

h is Planck's constant

Θ_ν is transmittance

$\Theta_{i,l}$ is the contribution to the transmittance in channel i due to absorption lines

I_i is the radiance value for the i^{th} channel

I_ν is radiance

k is the Boltzmann constant

κ_ν is the absorption coefficient

λ is wavelength

μ	is cos ψ
ν	is the wavenumber
N	is the number of data elements in an observation
P	is pressure
P_s	is surface pressure
ρ	is density
ρ_w	is water vapor density
r	is mixing ratio
$\underline{\underline{R}}$	is the eigenvector matrix
$\underline{\underline{R}}^T$	is its transpose
rms	is root mean square
s	is distance
T	is temperature (kinetic)
T_s	is surface temperature
τ_ν	is optical depth
v_i	is a parameter
v_i^*	is an estimated parameter
$W_{(p)}$	is precipitable water measured from the top of the atmosphere down to pressure level p
ψ	is zenith angle

1. INTRODUCTION

1.1 Objectives

The Defense Meteorological Satellite Program (DMSP) Block VD satellites will each have a Supplementary Sensor H (SSH) package with an infrared sounder having channels in the 18 to 30 μm absorption band of water vapor. The SSH package will also have channels in the 11 to 15 μm absorption band of carbon dioxide (CO_2) for temperature sounding and a single channel at 10 μm for sensing ozone. The objective of the work reported herein, conducted by *Environmental Research & Technology, Inc.*, (ERT), was to develop an algorithm for the extraction of moisture parameters from the water vapor channels data. The moisture parameters are to be used for the correction of sea surface temperature maps and temperature profiles obtained from satellite-borne infrared radiometers.

1.2 Summary of Results

The radiances for the eight water vapor channels on the DMSP/SSH package were simulated for cloud-free conditions using (1) the high resolution transmittance calculations provided by the Air Force Geophysics Laboratory* (McClatchey et al., 1973); (2) the temperature and water vapor profiles used for the transmittance calculations; and (3) the frequency dependences of each of the channel filters. Calculations were performed for a set of 220 atmospheric profiles selected by the Air Force Global Weather Central (Wachtmann, 1975) to be statistically representative of the expected range of temperature and moisture profiles.

The simulated radiances were inverted using a statistical multiple regression procedure (Gaut et al., 1972) to estimate total precipitable water and precipitable water profiles for the lower layers of the atmosphere. Inversions were made using combinations of water vapor channel and temperature profile data. Results for the estimation of total precipitable water are shown in Table 1. The ratio of variances is the

*Data tapes with calculated transmittance values for 220 atmospheric profiles were provided by Dr. R. B. McClatchey of AFGL.

TABLE 1

REDUCTION IN VARIANCE FOR TOTAL PRECIPITABLE WATER ESTIMATORS

Infrared Channel	Number of Temperature Levels	Ratio of Variances
8	5†	8.0
4**	5	8.1
7*	5	7.2
8	0	2.1
7*	0	1.2
4**	0	2.3
535 cm^{-1}	0	1.5
0	5	3.2
535 cm^{-1}	5	7.0

* Did not include 535 cm^{-1} channel

** 398, 410, 442 and 535 cm^{-1} channels

† 100, 920, 850, 700, and 500 mb temperature values

a priori variance of the entire data set divided by the residual variance after multiple regression analysis or the factor by which the variance was reduced.

Channel selection included or excluded the 18.7 μm (535 cm^{-1}) channel. This channel is not included on the first SSH flight model but will be available on succeeding SSH models. The four channels at 398, 410, 442, and 535 cm^{-1} were selected as an optimum subset of the full complement of eight channels. Finally, since the difference between using all eight channels and the first seven channels was large, the use of only the 535 cm^{-1} channel was explored.

The results listed in Table 1 show that the combination of eight water vapor channels plus the temperature data at five levels produced the best results; the use of the seven water vapor channels to be flown on the first SSH flight model without including temperature data produced no reduction in variance from the a priori value obtained using climatological data. Results obtained using only water vapor channel data and including the 535 cm^{-1} channel were intermediate between these cases. The incorporation of the 535 cm^{-1} channel with the temperature profile data significantly improved the estimate of total precipitable water over the use of the single infrared channel alone or the temperature data alone.

The results did not change when both the radiance and temperature values were perturbed by measurement noise. Design level noise of 0.25 ergs/sec was added to the radiance values and a 2° rms (root mean square) temperature uncertainty was used. The latter value is typical of the precision that can be accomplished from infrared temperature profile measurements under cloud-free conditions.

The details of the moisture parameter retrieval analysis are presented in this report. Section 2 describes the inversion problem and the statistical multiple regression procedure used in the analysis; Section 3 describes the simulation procedures; Section 4 provides a discussion of results; and Section 5 presents conclusions and recommendations. A description of the software and $\underline{\underline{D}}$ matrices for a sample set of inversions are given in the appendices.

2. THE INVERSION PROBLEM

2.1 The Radiative Transfer Equation

The upwelling thermal infrared radiation sensed by radiometers on the DMSP satellites originates from surface emission and from the atmosphere above the surface. In the absence of clouds, the radiance detected at the satellite may be calculated using the radiative transfer equation for an absorbing medium (Chandrasekhar, 1960):

$$I_\nu(o) = I_\nu(s)e^{-\tau_\nu(s)} + \int_o^s \kappa_\nu(x)\, B_\nu(T(x))e^{-\tau_\nu(x)}dx \qquad (2\text{-}1)$$

where

$I_\nu(x)$ is radiance at x along the path measured from the satellite

$\tau_\nu(x)$ is optical depth $= \int_o^s \kappa_\nu(y)dy$

$\kappa_\nu(x)$ is absorption coefficient

$B_\nu(T(x)) = \dfrac{c_1\nu^3}{(e^{c_2\nu/T} - 1)}$ = Planck radiance

s is distance to surface

λ is wavelength

ν is the wavenumber

T is temperature (kinetic)

$c_1 = 2hc$ = first Planck constant

$c_2 = hc/k$ = second Planck constant

h is Planck's constant

k is the Boltzmann constant

Using the hydrostatic equation and assuming that the surface radiates as a black body, this expression may be simplified to

$$I_\nu = B_\nu[T_s]e^{-\tau_\nu(Ps)} + \int_o^{P_s} B_\nu[T(P)]e^{-\tau_\nu(P)}\left(\frac{\kappa_\nu}{\rho\mu g}\right)dP \qquad (2\text{-}2)$$

where

$$\tau_\nu(P) = \int_o^P \frac{\kappa_\nu dP}{\rho\mu g}$$

ρ = $\rho(P)$ = density

P is pressure

P_s is surface pressure

T_s is surface temperature

g is acceleration due to gravity

μ is $\cos\psi$

ψ is zenith angle

and the atmosphere is assumed to be horizontally layered over a flat surface (plane parallel). Finally, noting that

$$d\tau = \kappa_\nu \frac{dP}{\rho\mu g}$$

the radiative transfer equation can be reduced to the familiar form

$$I_\nu = B_\nu[T_s]\,\Theta_\nu(P_s) - \int_o^{P_s} B_\nu[T(P)]\,\frac{d\Theta_\nu(P)}{dP}\,dP \qquad (2\text{-}3)$$

where

$\Theta_\nu = e^{-\tau_\nu}$ = transmittance

The three forms of the radiative transfer equation were explicitly presented to emphasize the complexity of the relationship between I_ν measured at the satellite and the atmospheric parameters of interest. Moisture parameters such as mixing ratio and precipitable water do not explicitly appear. In the 18 to 30 μm ($330\ cm^{-1} < \nu < 550\ cm^{-1}$) band the only important source of absorption is water vapor. The absorption coefficient depends upon the contributions of a number of rotational-vibrational absorption lines in the vicinity of ν. Following Burch

et al (1974), the absorption coefficient may be modeled as a sum of the contribution of nearby lines (local) and a continuum contribution contributed by the far wings of a large number of distant lines. The local pressure broadened lines may be described by the classical Lorentz line shape and the contribution of each line may be calculated given the frequency, width and intensity of each line. The Lorentz line shape does not adequately represent the actual line intensity more than 10 - 15 cm^{-1} from the line center. At larger frequency offsets, the contributions from a large number of distant lines becomes important and their contributions may be modeled as background continuum absorption.

The model for the absorption coefficient is given by:

$$\frac{\kappa_\nu}{\rho} = \frac{e}{\rho kT}\left[\sum_i C_i p + C_s e + C_n p\right] \qquad (2\text{-}4)$$

where

- e is the partial pressure of water vapor,
- C_s is the continuum coefficient for self broadening,
- C_n is the continuum coefficient for total pressure (nitrogen) broadening, and
- C_i are the contributions by lines at ν_i with the line width pressure dependence made explicit.

Noting that $e/T \propto \rho_w$, the water vapor density, Equation 2-4 may be represented by

$$\frac{\kappa_\nu}{\rho} = r[f_1(\nu,P,T) + r\, f_2(\nu,P,T)]$$

to make the dependence on mixing ratio, r, explicit. Now Equation 2-2 may be rewritten

$$I_\nu = B_\nu(T_s)e^{-\tau_\nu(P_s)} + \int_0^{P_s} B_\nu[T(P)]e^{-\tau_\nu(P)}\, r(f_1 + rf_2)\frac{dP}{\mu g} \qquad (2\text{-}5)$$

where

$$\tau_\nu = \int_o^P r(f_1 + rf_2)\frac{dP}{\mu g}$$

The dependence of the measured radiance on mixing ratio is highly nonlinear. The optical depth is a temperature and pressure weighted integral of the mixing ratio plus a term with a second order dependence on mixing ratio. The radiance values have a further nonlinear dependence on the weighted integral of mixing ratio through the exponential function. Equation 2-5 is a nonlinear equation for r when I_ν is given. To obtain information about r or about precipitable water, W,

$$W_{(P)} = \int_o^P \frac{rdP}{g}$$

the equation must be inverted.

2.2 Statistical Parameter Inversion Method

The integral equation (Equation 2-5) is highly nonlinear in r. Smith and Howell (1971) attempted to invert this equation using an iterative technique. To be sucessful, the iterative solution should take into account the variations of the weighting functions with the mixing ratio profile and temperature profile. For the analysis of temperature profiles using iterative techniques such as the minimum information technique, the variation of the weighting functions with the parameter of interest, temperature, is assumed to be small and a fixed weighting function can be assumed. This is not possible for the inversion of water vapor data. The result is a lengthy, time consuming process which, in the end, may not converge to the desired result due to the non-uniqueness of the solution.

The Statistical Parameter Inversion Method developed by ERT (Gaut et al., 1972) bypasses the requirement for the lengthy iterative procedure for the inversion of the radiative transfer equation by using multiple regression techniques. Multiple regression procedure has been used by many investigators for the inversion of the radiative transfer equation. Recently, Smith and Woolf (1976) described a procedure nearly

identical to the one used by Gaut et al. (1972) for the inversion of Nimbus-6 data to generate temperature and mixing ratio profiles. As applied, a multiple regression analysis is performed using radiance data or, in their absence, simulated radiances as the independent set of variates and the desired parameters as the dependent set. A linear relationship is assumed between the dependent and independent sets and the least square and best estimate coefficients relating the two sets are determined which minimize the differences between the estimated and observed values. This procedure selects the most probable set of parameters from the infinite set of parameters that could have produced the same radiance values.

Let v_i be the i^{th} parameter, say $W_{(P)}$, and d_j be the j^{th} element of a measured data set, then the assumed relationship is

$$v_i^* = \sum_{j=1}^{N} D_{ij} d_j$$

which, in matrix notation, is

$$\underline{v} = \underline{\underline{D}}\,\underline{d}$$

where

v_i^* is the estimated parameter,

D_{ij} are the elements of a linear operator $\underline{\underline{D}}$ relating d_j to v_i^*, and

N is the number of data elements in an observation.

The problem is to determine the elements of the linear operator such that the variance of the difference between v_i and v_i^* is a minimum (least square minimum error). The elements of the linear operator can be estimated using multiple regression techniques and simultaneous sets of observations (or simulations) of $\underline{v}$ and $\underline{d}$. The elements $\underline{\underline{D}}$ then minimize the error for the sets of observations. For use as an estimation procedure with a new set of observations, the elements of $\underline{\underline{D}}$ will only provide minimum variance if the statistical properties of both the original and new sets are identical. This is usually taken on faith if simultaneous $\underline{v}$ and $\underline{d}$ elements are not available or can be tested if they are available.

The Statistical Parameter Estimation Method first determines the empirical orthogonal functions that best represent the data elements. The data are then represented by a truncated set of the empirical orthogonal functions to minimize the effect of noise and redundant observations. The latter set is used in a classical regression analysis to determine the $\underline{\underline{D}}$ matrix elements. The calculations are made using a modified $\underline{d}'$ vector with the first element set to unity and the remaining elements equal to the departures from their expected mean values normalized by the expected mean value

$$\{d_i'\} = \left\{ \frac{1, d_{i-1} - \langle d_{i-1} \rangle}{\langle d_{i-1} \rangle} \right\}$$

where the $\langle\ \rangle$ operation represents averaging over the number of observations in the set used to generate the D matrix. The correlation matrix, $\underline{\underline{C}}\ (\underline{d}', \underline{d}')$ where $C_{ij} = \langle d_i' d_j' \rangle$, is generated using the values for $\underline{d}'$ and is diagonalized to determine both its eigenvalues and eigenvectors. The eigenvectors are the empirical orthogonal functions for the data elements and the eigenvalues give the amount of the variance represented or explained by each eigenvector (Lorentz, 1956).

The transpose of the eigenvector matrix ($\underline{\underline{R}}^T$) is used to transform the modified data vector $\underline{d}'$ to a new data vector $\underline{d}'' = \underline{\underline{R}}^T \underline{d}'$ which may be truncated to provide a best representation of the data vector for use in the regression analysis. Using the truncated set,

$$\underline{\underline{D}}'' = \underline{\underline{C}}(\underline{v}, \underline{d}'')\ \underline{\underline{C}}^{-1}(\underline{d}'', \underline{d}'')$$

The $\underline{\underline{D}}'$ matrix for use in estimating $\underline{v}$ is then $\underline{\underline{D}}' = \underline{\underline{D}}'' \cdot \underline{\underline{R}}^T$. The $\underline{\underline{D}}$ matrix calculated in this manner minimizes sensitivity to noise and correlation between data elements; the correlated data elements being represented by a single component of the empirical orthogonal function set (Gaut et al, 1972; Smith and Woolf, 1976).

3. SIMULATION OF RADIANCES

3.1 Band Pass Filters

The use of the $\underline{\underline{D}}'$ matrix for the inversion of infrared sounder measurements first requires the availability of both data and simultaneously observed parameters for the generation of a $\underline{\underline{D}}'$ matrix. In the absence of actual observations, simulated data must be used. The radiances to be observed in each of the channels of the DMSP/SSH sounder are not single frequency observations as implied in the equations of Section 2.1 but are spaced over the frequency band defined by the instrument filters.

Table 2 describes the frequency bandpass characteristics of the F channels of the first flight model water vapor sounding (Barnes Engineering Co., 1975) and of the eighth channel to be included on the subsequent flight models. The numbers 1 to 8, given in Table 2, are used to refer to the channels. Their bandpass characteristics in terms of energy throughput or transmission are displayed on Figure 1. The data on this figure were compiled from measurements at 0.5 cm^{-1} spacings provided by the manufacturer (Barnes Engineering Co., 1975) and were used to define the response of each of the sounder channels. Although the full system frequency response as well as the filter response were measured by the manufacturer, digitized data were available for the filters and were used for the simulation. As shown in Table 2, the differences between using the two sets of data, as calculated by the manufacturer and as calculated from the digitized filter data plotted on Figure 1 are small. The data for channel 8 were obtained from measurements on a similar channel filter on the sensor on satellite DMSP-6530.

The radiances to be measured on the satellite are related to the theoretical values described in Section 2.1 by

$$I_i = \int_0^\infty g_i(\nu) I_\nu d\nu$$

where g_i is the transmission function for the i^{th} channel.

TABLE 2

FILTER DATA FOR DMSP/SSH WATER VAPOR CHANNELS

Channel	Spectral Band	Provided by Manufacturer			Calculated from Filter Data		
		Center Wavelength (cm^{-1})	Half Width (cm^{-1})	Tenth Width (cm^{-1})	Center (cm^{-1})	Half Width (cm^{-1})	Tenth Width (cm^{-1})
1	F8-Filter	353.84	11.55	20.36	353.78	11.55	18.28
	F8-System	354.22	11.62	20.19			
2	F1-Filter	356.27	14.96	23.58	356.67	14.77	22.06
	F1-System	356.86	14.07	23.12			
3	F7-Filter	373.36	11.17	23.00	373.46	11.17	20.13
	F7-System	373.56	11.13	22.86			
4	F2-Filter	398.15	10.88	19.60	398.15	10.88	17.53
	F2-System	398.05	10.67	19.18			
5	F6-Filter	410.08	13.73	22.02	409.83	13.69	19.96
	F6-System	409.88	13.90	22.40			
6	F3-Filter	418.29	19.12	28.06	418.96	19.12	25.74
	F3-System	418.30	19.16	28.29			
7	F4-Filter	441.94	18.43	36.81	442.19	18.43	33.09
	F4-System	441.67	17.63	35.65			
8					534.35	11.55	18.43

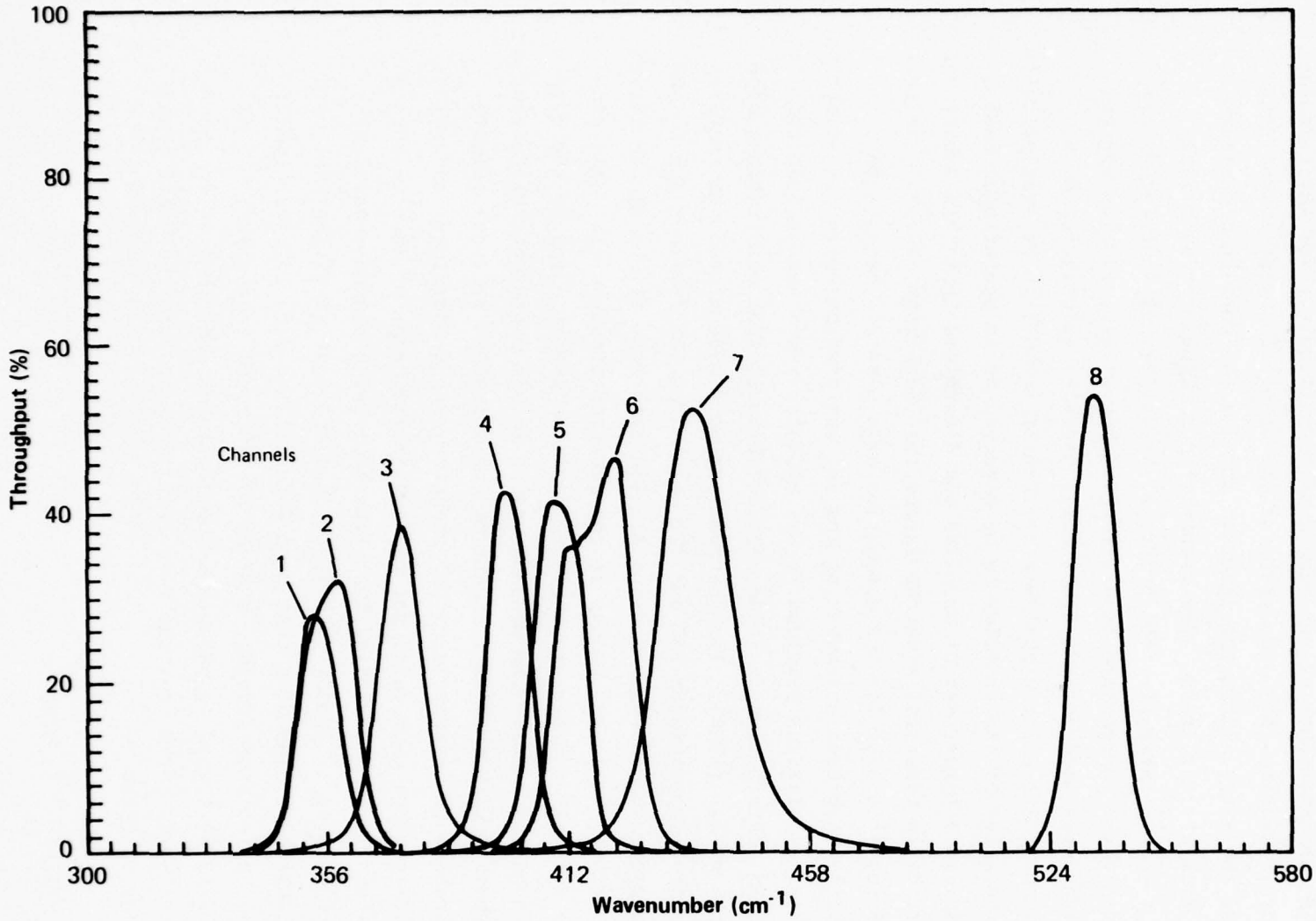

Figure 1 Wavenumber Dependence of the SSH Instrument Filters

3.2 Calculations of Transmittance

The transmittance values needed at each frequency for the calculation of I_i require the calculation of the absorption coefficient for each of the lines within the interval and for the continuum contributions from distant lines. The transmittance values for each line $\Theta_\nu(p) = e^{-\tau_\nu(P)}$ were provided by Dr. R. McClatchey of AFGL for 0.1 cm^{-1} increments and 12 pressure levels (McClatchey et al., 1973). The calculations were made for 220 atmospheric profiles selected by R. F. Wachtmann of Air Force Global Weather Center (AFGWC) to be statistically representative of the profiles to be expected on an operational basis. He compiled a larger set of profiles and determined that this subset was statistically identical with the larger set (Wachtmann, 1975). The set, therefore, is useful for the estimation of a $\underline{\underline{D}}$ matrix because the statistical representativeness of the set was considered in its selection.

The calculations provided by Dr. McClatchey did not include the continuum contributions. These were established from observations made by Burch et al. (1974). The observations were made at two temperatures in spectral gaps between 337 and 822 cm^{-1}. The observations for C_s and C_n are presented in Figures 2 and 3. The data were fit by smooth curves that matched the lowest values at the reported frequencies. This procedure was followed because the data could be contaminated by the edges of neighboring lines. The minimum values should represent the continuum contribution with the least amount of contamination by local effects. The curves were separately established for each temperature, and values were scaled from each curve for the center frequency of each channel and tabulated (Table 3). Noting that line broadening can be modeled as proportional to T^n (Goody, 1964), the two temperature values were used to establish a value of n that best fits all the data for each coefficient. For self-broadening, n = -2; for nitrogen broadening, n = +2. These data were used to calculate the continuum contribution to the transmittance. From Equation 2-3, it is evident that the total transmittance is given by

$$\Theta_{i(P)} = \Theta_{i,\ell(P)} \cdot \Theta_{i,c(P)}$$

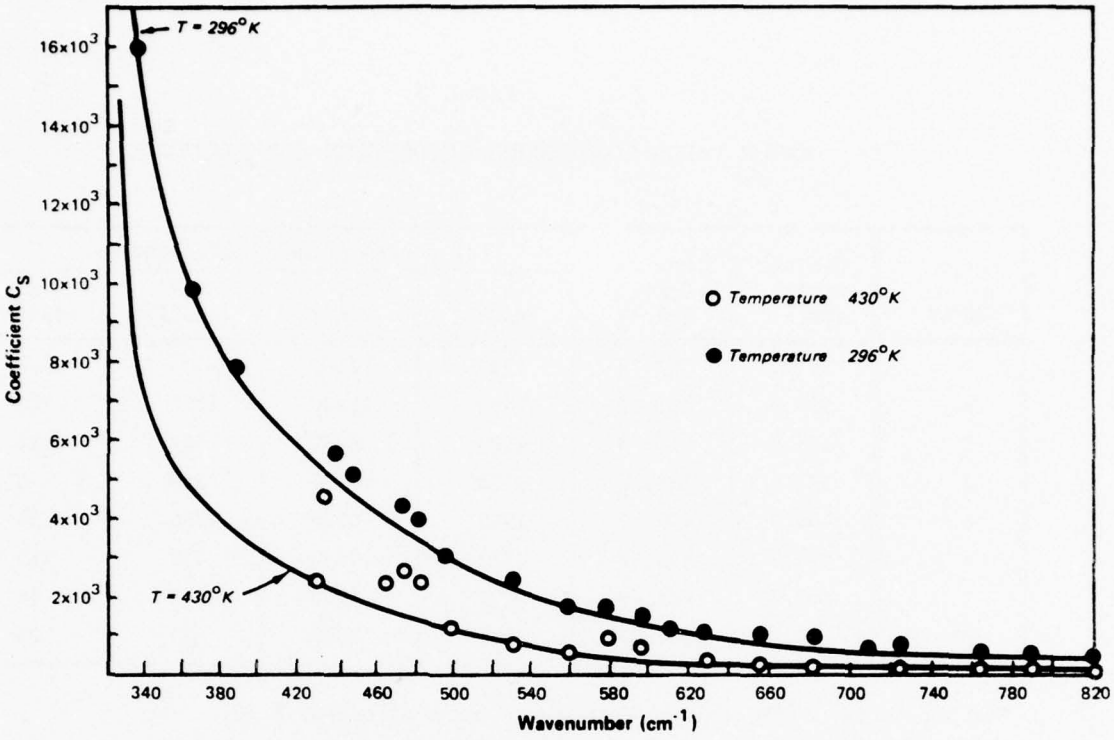

Figure 2 Water Vapor Continuum Absorption Coefficients (Self Broadening Term)

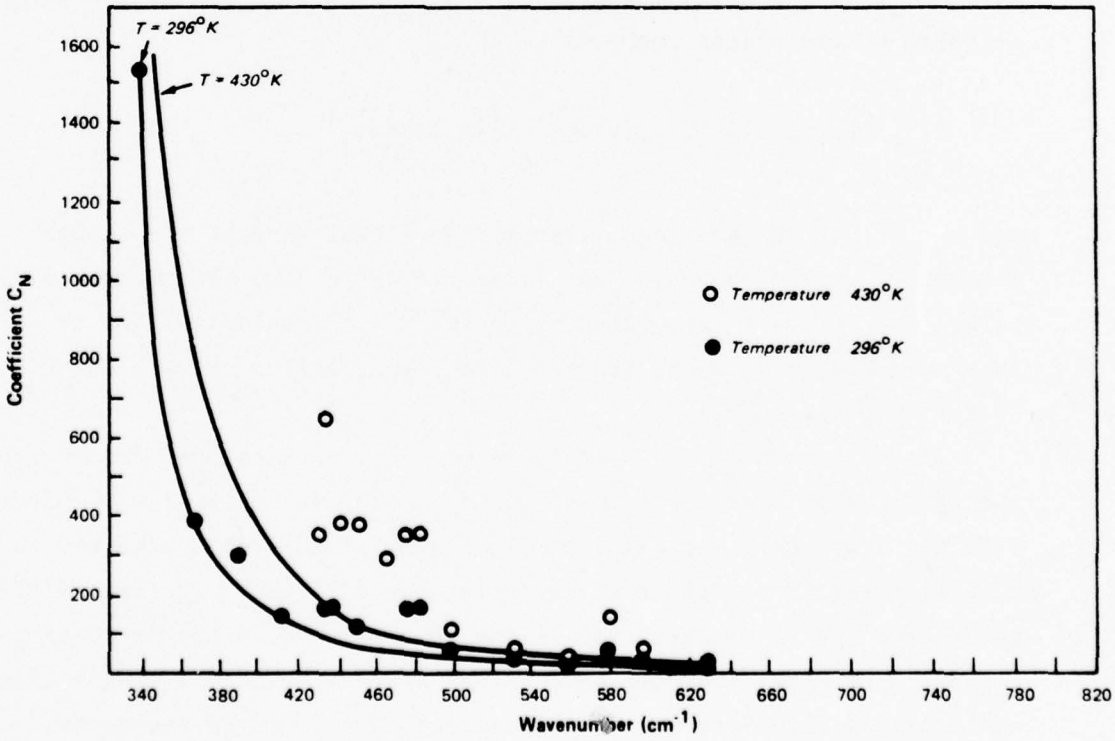

Figure 3 Water Vapor Continuum Absorption Coefficients (N_2 Broadening)

TABLE 3

WATER VAPOR CONTINUOUS ABSORPTION COEFFICIENTS

Channel	Nominal Center (cm^{-1})	Optical Center (cm^{-1})	Absorption Coefficient			
			C_s (430°K)	C_s (296°K)	C_n (430°K)	C_n (296°K)
1	353.0	353.78	5757	12150	1245	590
2	359.0	356.67	5450	11400	1055	500
3	373.5	373.46	4194	8850	654	310
4	397.5	398.15	3270	6900	369	175
5	409.0	409.83	2962	6250	285	135
6	423.0	418.96	2725	5750	232	110
7	441.0	442.19	2227	4700	137	65
8*	534.5	534.35	972	2050	53	25

*Not on Flight I/SSH (Filter Response Function from DMSP-6530)

where $\Theta_{i,\ell}$ is the transmittance for the lines within the filter bandpass weighted by the filter response

$$\Theta_{i,\ell}(P) = \left(\int \Theta_{\nu}(P) g_i(\nu) d\nu\right) \cdot \left(\int g_i(\nu) d\nu\right)^{-1}$$

and $\Theta_{i,c}(P)$ is the continuum transmittance evaluated at the center frequency for the channel. The filter weighted line transmittance values $\Theta_{i,\ell}(P)$ were calculated using the $\Theta_{\nu,\ell}(P)$ values at 0.1 cm^{-1} intervals and by a second order spline interpolation between the 0.5 cm^{-1} filter response values.

The continuum calculations were made for each channel center frequency using 35 pressure levels equally spaced in units of $P^{2/7}$ between 0.01 and 1,000 mb. The values of T, P and r required to make the calculations were the average values between the layers. The transmittance values for the lines were also spline interpolated to the 35 pressure levels. The total transmittance values were calculated for each channel and pressure level for use in calculating the simulated radiances.

Weighting functions were calculated for several of the profiles to display the results of the transmittance calculations. The weighting functions for the Planck radiance (Equations 2-1 and 2-3) were calculated by the weighting function

$$\frac{d\Theta_i}{dH} = \frac{d\Theta_i}{d(\ln P)}$$

Weighting functions for all the channels for a tropical summer atmosphere are displayed on Figure 4. With the exception of channel 8, all the weighting functions peak at 500 mb or above. Although these weighting functions are not the coefficients of precipitable water or of mixing ratio, the parameters to be sensed (Smith and Howell, 1971), they show that only the Planck radiances in the upper layers of the atmosphere contribute to the radiance values. As displayed, the weighting functions contain the water vapor information. These functions show that only water vapor above 500 mb can be sensed for this profile.

A subset of four channels were selected that had weighting functions that peaked at different heights in the lower atmosphere. Weighting functions for channels 4, 5, 7 and 8 at 398, 410, 442 and 534 cm^{-1}, respectively, are displayed for two widely different atmospheres on Figures 5 and 6. Figure 5 is for the same atmospheric profile as Figure 4, tropical summer. Figure 6 represents an arctic winter profile. These data show that channels 4, 5 and 7 peak at the same height for the moist, warm tropical summer profile. The weighting functions peak at much lower heights for the cold, dry arctic winter profile. In the latter case, channel 8 should provide useful information down to the surface. These data display the wide variability possible for the product $\kappa_\nu e^{-\tau_\nu(P)}$ (see Equation 2-1).

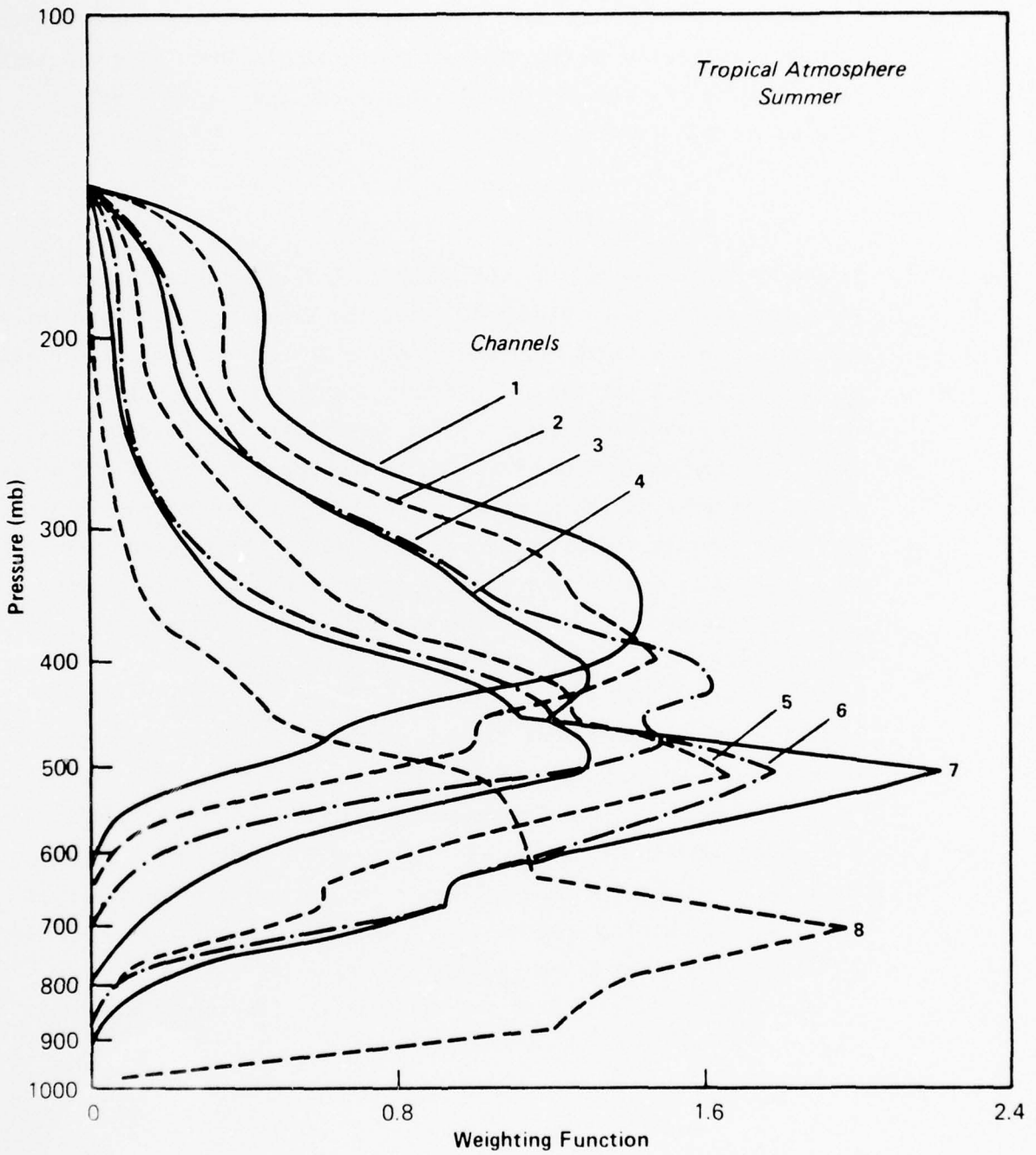

Figure 4 Pressure Dependence of the Weighting Functions for the Planck Radiance for Each Water Vapor Channel

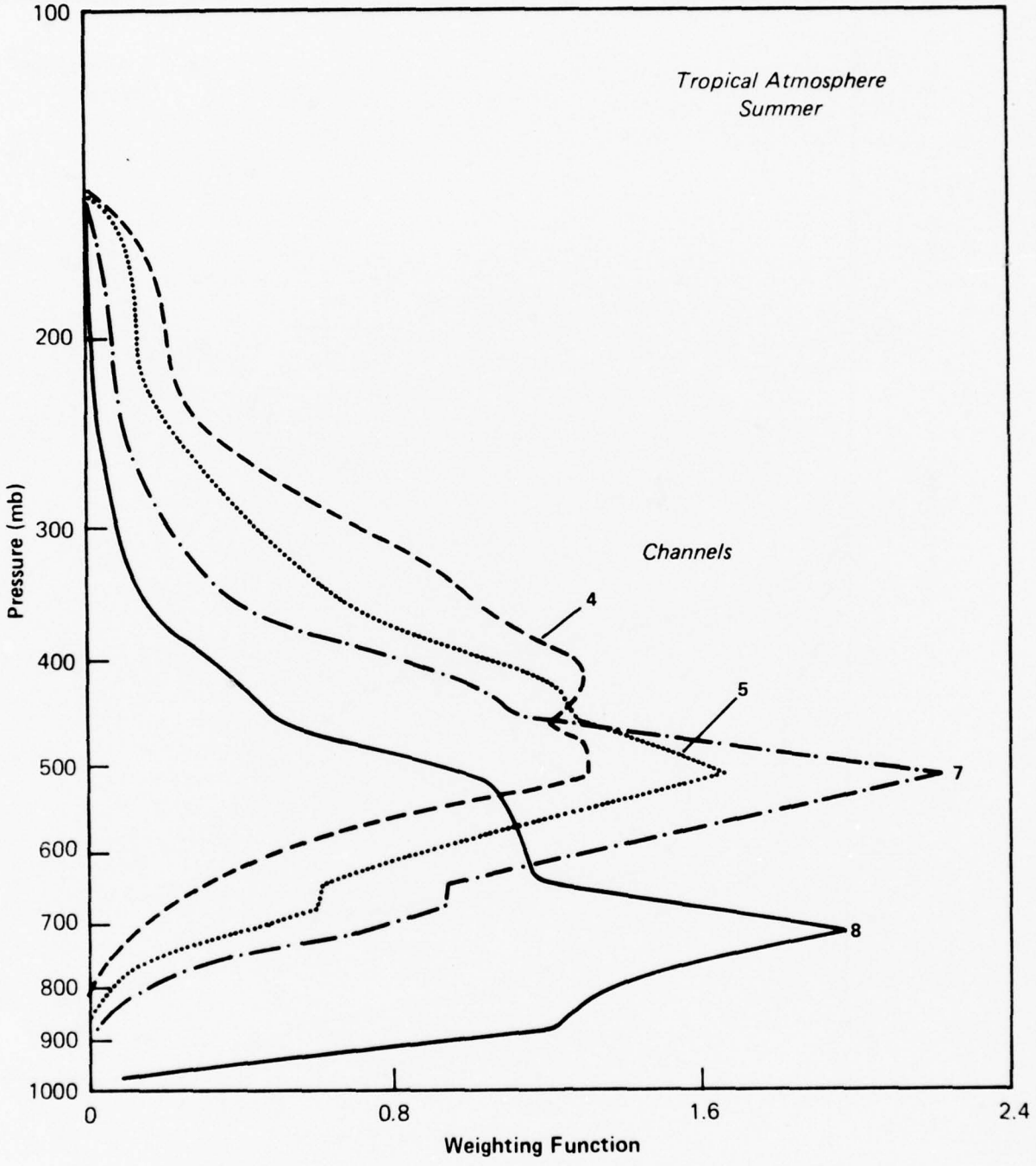

Figure 5 Pressure Dependence of the Weighting Functions for the Planck Radiance (Tropical Summer Atmosphere)

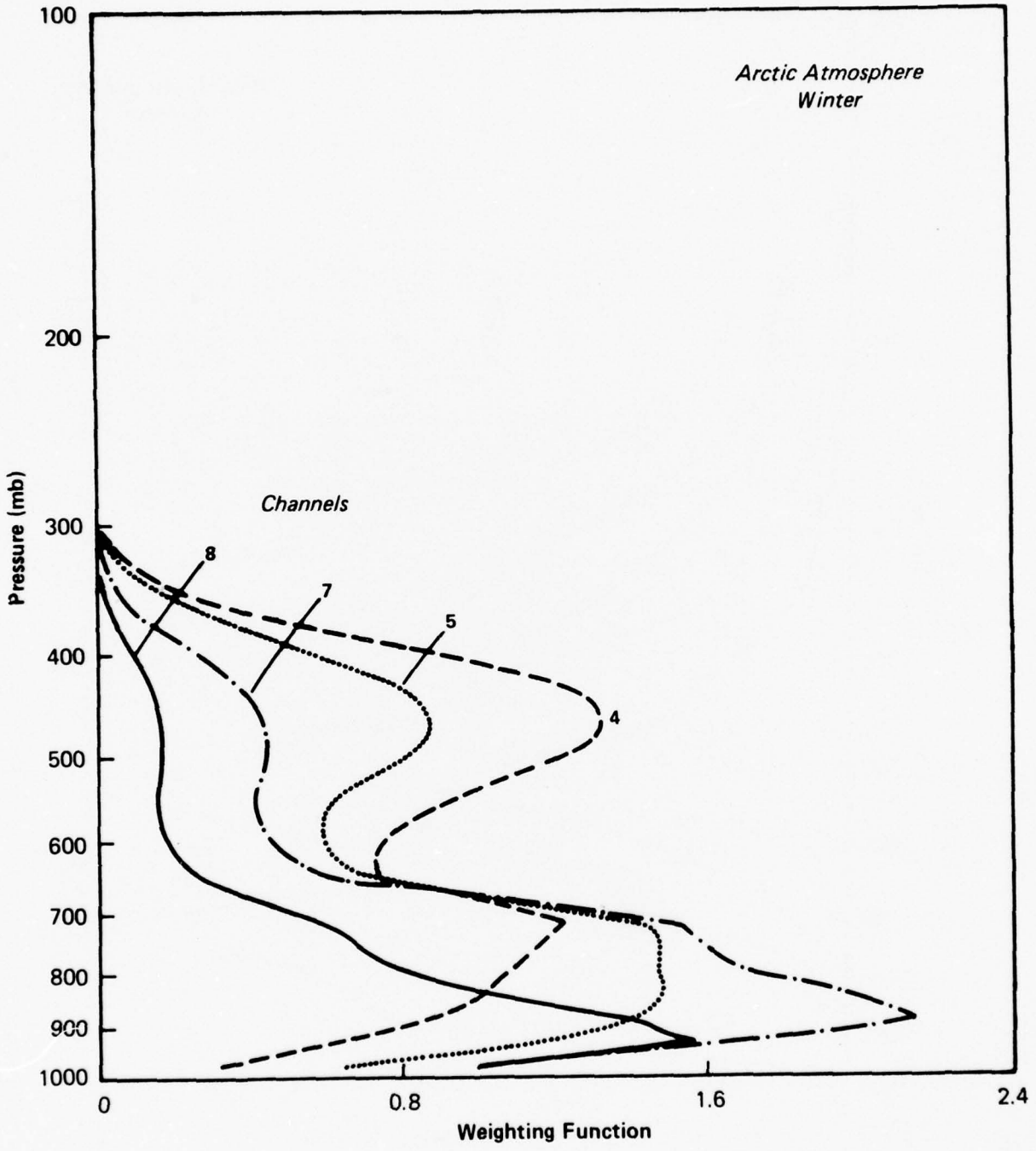

Figure 6 Pressure Dependence of the Weighting Functions for the Planck Radiance (Arctic Winter Atmosphere)

3.3 Radiance Calculations

The radiance values, I_e, were calculated using the 35 pressure levels and evaluating the Planck radiances for the layers between the radiance levels. From Equation 2-3, it is evident that a surface temperature must be specified to calculate the surface emission for use in the radiative transfer equation. Surface temperature measurements were not provided with the 220 atmospheric profiles. Surface temperature values for use in the equation were randomly generated to be within 1.5° rms of the 1,000 mb temperature value. The surface is assumed to be at 1,000 mb and to have unity emissivity.

The radiance calculations were made for each of the 220 profiles. Calculated radiance values for the two samples, the arctic winter and tropical summer profiles, are displayed on Figure 7. These data show large variations between the observations. The data are of the same order of magnitude as the arctic and tropical observations reported by Hanel and Conrath (1970).

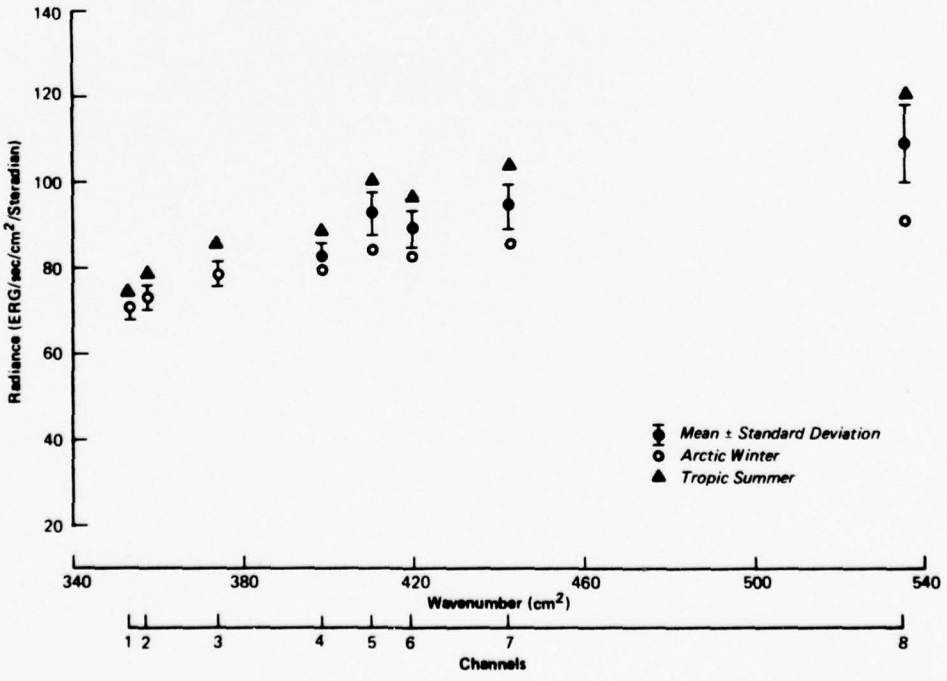

Figure 7 Radiance Estimate Summary for the 220 Atmospheric Profiles and Examples for Arctic Winter and Tropic Summer

4. ANALYSIS

4.1 Sample Variability

The set of 220 simulated radiances and their associated atmospheric profiles comprise the data and parameter set used for the generation of the $\underline{\underline{D}}$ matrix. The utility of different retrieval algorithms using different channels and combinations of channel radiance values and temperature values is measured by the factor by which the a priori or climatological variance of the parameter is reduced. The variance values and covariances required to generate the $\underline{\underline{D}}$ matrices used for the retrieval of precipitable water were calculated using the entire set of 220 atmospheric profiles. The profiles were selected from a larger set and constrained to have the same statistical properties as the larger set (Wachtmann, 1975). The resultant data set represents a number of profiles from different latitude regions and months of the year as shown in Table 4. The mean and standard deviation of the calculated radiances for this data set are shown on Figure 7.

TABLE 4

DISTRIBUTION OF SOUNDINGS BY LATITUDE AND NORTHERN HEMISPHERE MONTHS

Month	Latitude					
	1-15°	15-30°	30-45°	45-60°	60-75°	75-90°
Jan	16(10)	18	14	37	20	13
Feb	10(4)	18	17	25	10	15
Mar	14(4)	20	17	18	9	10
Apr	8(8)	17	12(2)	29	18	14
May	18(10)	21	24(2)	12	15	16
Jun	16(8)	26	21(4)	24	22	10
Jul	17(11)	23	24(2)	23(3)	15(9)	15(4)
Aug	15(7)	20	20	23(7)	25(5)	12
Sep	10(10)	12	15	0	6(4)	4
Oct	20(9)	16	20	23	10	10
Nov	13(7)	18	16	21	10	10
Dec	19(10)	16	16	44	10	6

*The numbers in parentheses represent that part of the total taken in the southern hemisphere. Southern hemisphere soundings are counted for the month six months out of phase of the observation month in order to represent seasonal distribution.

The moisture parameter selected to test the inversion algorithms for the simulated data are the precipitable water values for five pressure levels between 1,000 and 500 mb. The precipitable water is defined by Equation 2-6. The total precipitable water is the value for 1,000 mb pressure. This value is of most interest for sea surface temperature mapping and was used by Cogan and Willand (1975) as an independent variable in the procedure for estimating the temperature deficit for the correction of the sea surface values. Similarly, the precipitable water values for different pressure levels are required to estimate corrections for the transmission functions used in the retrieval of temperature profile data from the CO_2 sounder channels' data. The mean and standard deviations of precipitable water are depicted on Figure 8 and are listed in Table 5. From the table, it is evident that the a priori or climatological standard deviation of precipitable water varies from 60 to 80 percent of the mean depending upon the pressure level. The individual tropical summer and arctic winter profiles used in the radiance calculations depicted in Figure 7 are displayed in Figure 8.

The precipitable water values are not all independent parameters. The first three eigenvectors in an empirical orthogonal function representation of the parameter set explain 99.91 percent of the variance. A similar analysis for the eight water vapor channels shows that the radiances are highly correlated. The first three eigenvectors in an empirical orthogonal function representation of the radiances explain 99.966 percent and the first four eigenvectors explain 99.997 percent. The temperature values at the same pressure levels used for precipitable water have the mean and variance values listed in Table 6. Again, an empirical orthogonal function representation of the temperature data shows that only two eigenvectors are required to explain 99.97 percent of the variance. These results show that both the data elements are highly correlated and the parameter elements are also highly correlated. This means that the number of independent pieces of information in an observation is significantly smaller than the number of sounder channels.

TABLE 5

A PRIORI PRECIPITABLE WATER PARAMETERS

Pressure (mb)	Mean (gm/cm^2)	Variance $(gm/cm^2)^2$	Standard Deviation (gm/cm^2)	Standard Deviation Percent of Mean
1000	2.9	2.7	1.6	57
920	2.0	1.3	1.2	59
850	1.5	0.78	0.88	61
700	0.66	0.19	0.44	66
500	0.14	0.012	0.11	77

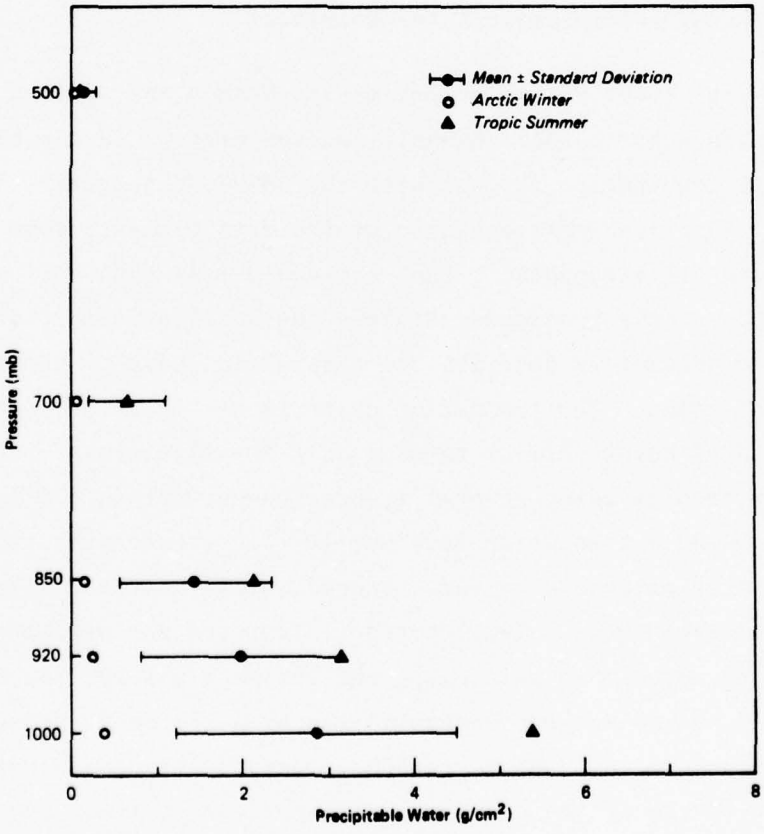

Figure 8 Precipitable Water Estimate Summary for the 220 Atmospheric Profiles and Examples for Arctic Winter and Tropic Summer

TABLE 6

TEMPERATURE VALUES

Pressure (mb)	Mean (°K)	Variance $(°K)^2$	Standard Deviation (°K)
1000	287.7	175	13.2
920	285.0	145	12.1
850	282.3	128	11.3
700	275.1	92	9.6
500	259.5	85	9.2

4.2 Results of Precipitable Water Retrieval

The Statistical Parameter Estimation Method was applied to a number of combinations of sounder channels and temperature levels to determine the optimum combination for use with the DMSP/SSH sounder. The empirical orthogonal function representation of the data elements were truncated to eliminate all eigenvectors that explained less than 0.01 percent of the variance. This procedure retained the smallest number of elements required to adequately describe the data while reducing the effects of measurement noise. The truncation criteria was selected to eliminate the effects of noise while retaining only the significant data. A comparison of results using several truncation criteria are displayed in Table 7. Using a truncation level of 10^{-3} (0.1 percent), the variance for total precipitable water was reduced only 30 percent. Reducing the truncation level to 10^{-4} (0.01 percent) improved the estimate of total precipitable water. In this case, the variance was reduced by 53 percent both with and without contamination by measurement noise. The measurement noise was used to randomly perturb the data elements prior to the generation of the $\underline{\underline{D}}$ matrix. The percent variance represented by the noise of 0.002, which is rejected by the selected truncation level. A lower truncation level would produce noise sensitive results.

TABLE 7

COMPARISON OF RESIDUAL ERRORS USING DIFFERENT TRUNCATION LEVELS

8 SOUNDER CHANNELS

Pressure (mb)	Mean Precipitable Water (g/cm^2)	A Priori Standard Deviation (g/cm^2)	Residual Standard Deviation			Percent Variance Reduction		
			10^{-3} No Noise (g/cm^2)	10^{-4} No Noise (g/cm^2)	10^{-4} 0.25 erg/sec Noise (g/cm^2)	10^{-3} No Noise (%)	10^{-4} No Noise (%)	10^{-4} 0.25 erg/sec Noise (%)
1000	2.9	1.6	1.4	1.1	1.1	29	53	53
920	2.0	1.2	1.0	0.84	0.84	21	47	47
850	1.5	0.88	0.80	0.66	0.66	17	44	43
700	0.66	0.44	0.41	0.34	0.35	10	37	37
500	0.14	0.11	0.10	0.081	0.081	20	42	42

A number of sounder channel and temperature level parameters were used in the analyses of water vapor retrievals. Temperature was included as a data element because it determines the maximum value of precipitable water that the atmosphere can carry. It is often noted that relative humidity values vary over a narrow range. The mixing ratio values, therefore, should be highly correlated with the temperature values. Since the precipitable water is dominated by the contributions of the mixing ratio at the lowest level used in the calculation, the layer temperature value and precipitable water value should be highly correlated. This was true for the 220 sample profile set as indicated in Table 8. The correlations between temperature and precipitable water ranged from 0.5 to 0.8. The correlations between precipitable water and radiance values were smaller, ranging from 0.0 to 0.6.

A subset of four infrared sounder channels were also used for the estimation of precipitable water. Channels 4, 5, 7 and 8 (398, 410, 441 and 535 cm^{-1}) were selected as having the highest correlation with precipitable water (Table 8) and the largest differences in weighting functions. A subset of the original data set was selected as a method for operationally reducing the complexity of precipitable water retrieval algorithms.

The results of Statistical Parameter Estimation Method retrievals for each of the channel-temperature level combinations are presented in Tables 9 through 13. The data on each table are for a single precipitable water parameter. The results show that reductions in variance of 80 to 90 percent are possible using temperature data at four or five levels and at least one infrared sounder channel. The differences between the use of one or more sounder channels are small. The use of temperature only data provides a 70 percent reduction in variance for total precipitable water but using temperature in the lower levels only is not as useful for precipitable water for levels above 700 mb. Sounder data only is most useful when channel 8 is included but no reduction in variance (at the 0.05 significance level) occurs when channel 8 is not included.

TABLE 8

CORRELATION COEFFICIENTS FOR PARAMETER AND DATA ELEMENTS

Parameter	Data												
	Temperature					Radiance							
	$T_{(1000)}$	$T_{(920)}$	$T_{(850)}$	$T_{(700)}$	$T_{(500)}$	IR1	IR2	IR3	IR4	IR5	IR6	IR7	IR8
$W_{(1000)}$	0.79	0.80	0.80	0.77	0.80	0.19	0.25	0.33	0.35	0.40	0.39	0.43	0.59
$W_{(920)}$	0.73	0.75	0.76	0.74	0.76	0.15	0.20	0.26	0.28	0.31	0.31	0.35	0.51
$W_{(850)}$	0.69	0.72	0.73	0.71	0.73	0.12	0.16	0.22	0.23	0.25	0.26	0.29	0.46
$W_{(700)}$	0.59	0.63	0.65	0.64	0.67	0.04	0.06	0.10	0.11	0.13	0.13	0.17	0.34
$W_{(500)}$	0.52	0.56	0.59	0.59	0.63	-0.17	-0.14	-0.08	-0.05	0.07	0.02	0.08	0.30

TABLE 9

TOTAL PRECIPITABLE WATER RETRIEVAL $W_{(1000)}$

Channel	Temperature Levels (mb)	Standard Deviation of Residuals (gm/cm^2)	Ratio of Variance	Percent Reduction in Variance (%)
1-8	1000-500	0.58	8.0	87
1-8	1000-700	0.61	7.1	86
1-7	1000-500	0.61	7.2	86
4,5,7 & 8	1000-500	0.57	8.1	88
8	1000-500	0.62	7.0	86
No	1000-500	0.92	3.2	69
1-8	No	1.1	2.1	53
1-7	No	1.1		
4,5,7 & 8	No	1.1	2.3	56
4,5 & 7	No	1.5	1.2	17
8	No	1.3	1.5	35

TABLE 10

920 mb PRECIPITABLE WATER RETRIEVAL $W_{(920)}$

Channel	Temperature Levels (mb)	Standard Deviation of Residuals (gm/cm^2)	Ratio of Variance	Percent Reduction in Variance (%)
1-8	1000-500	0.40	8.5	88
1-8	1000-700	0.42	7.5	87
1-7	1000-500	0.43	7.2	86
4,5,7 & 8	1000-500	0.39	8.6	88
8	1000-500	0.43	7.3	86
No	1000-500	0.73	2.6	61
1-8	No	0.84	1.9	47
1-7	No	1.1	1.1	11
4,5,7 & 8	No	0.82	2.0	50
4,5 & 7	No	1.1	1.1	11
8	No	1.0	1.4	26

TABLE 11

850 mb PRECIPITABLE WATER RETRIEVAL $W_{(920)}$

Channel	Temperature Levels (mb)	Standard Deviation of Residuals (gm/cm^2)	Ratio of Variance	Precent Reduction in Variance (%)
1-8	1000-500	0.28	9.8	90
1-8	1000-700	0.30	8.5	88
1-7	1000-500	0.32	7.7	87
4,5,7 & 8	1000-500	0.28	10.0	90
8	1000-500	0.31	8.2	88
No	1000-500	0.59	2.3	56
1-8	No	0.66	1.8	44
1-7	No	0.85	1.1	8
4,5,7 & 8	No	0.64	1.9	47
4,5 & 7	No	0.85	1.1	8
8	No	0.78	1.3	21

TABLE 12

700 mb PRECIPITABLE WATER RETRIEVAL $W_{(700)}$

Channel	Temperature Levels (mb)	Standard Deviation of Residuals (gm/cm^2)	Ratio of Variance	Percent Reduction in Variance (%)
1-8	1000-500	0.12	13.3	92
1-8	1000-700	0.13	10.6	91
1-7	1000-500	0.15	8.8	89
4,5,7 & 8	1000-500	0.12	13.6	93
8	1000-500	0.13	11.0	91
No	1000-500	0.32	1.8	46
1-8	No	0.34	1.6	37
1-7	No	0.43	1.0	3
4,5,7 & 8	No	0.34	1.7	40
4,5 & 7	No	0.43	1.0	3
8	No	0.41	1.1	12

TABLE 13

500 mb PRECIPITABLE WATER RETRIEVAL $W_{(500)}$

Channel	Temperature Levels (mb)	Standard Deviation of Residuals (gm/cm^2)	Ratio of Variance	Percent Reduction in Variance (%)
1-8	1000-500	0.037	8.5	88
1-8	1000-700	0.042	6.5	85
1-7	1000-500	0.039	7.7	87
4,5,7 & 8	1000-500	0.037	8.4	88
8	1000-500	0.044	5.8	83
No	1000-500	0.083	1.7	41
1-8	No	0.081	1.7	42
1-7	No	0.10	1.1	8
4,5,7 & 8	No	0.081	1.7	43
4,5 & 7	No	0.10	1.1	8
8	No	0.10	1.1	9

4.3 Applications

The water vapor retrieval algorithm using both infrared and temperature profile data is capable of estimating total precipitable water with an rms error of less than 0.6 gm/cm^2. Shen and Smith (1972) estimated that the uncertainty in the estimation of total precipitable water achieval with the SIRS-B sounder was 0.6 gm/cm^2, the same as estimated for the DMSP/SSH sounder using the established regression procedure and both sounder and temperature data. The inversions may be made using the matrix operation $\underline{V} = \underline{\underline{D}}\,\underline{d}$ where the $\underline{\underline{D}}$ matrix elements are listed in Appendix 2. Since the 220 element data set was generated using statistically representative samples, the $\underline{\underline{D}}$ matrices generated using the simulated radiance values are applicable for operational use. The $\underline{\underline{D}}$ matrices generated in this fashion may not be the best for operational use in that the radiances are simulated, not measured, and possible errors in the model can affect the results. In practice, $\underline{\underline{D}}$ matrices generated using simultaneous cloud-free satellite observations and profile measurements are to be preferred.

The water vapor correction technique, described by Cogan and Willand (1975), relies upon the use of the total precipitable water as a predictor of temperature deficit. For a $W_{(1000)}$ estimation with a 0.6 gm/cm^2 rms error, the uncertainty in the prediction of the temperature deficit is less than 0.6°K. From the analysis presented by Cogan and Willand, the uncertainty in the estimation of sea surface temperature would be less than 1°K rms.

The procedure used for the extraction of precipitable water is applicable to cloud-free radiance observations. Temperature profile estimates with rms errors of less than 2°K are required for making estimates with less than 0.6 gm/cm^2 rms error in $W_{(1000)}$. These may be obtained from the CO_2 temperature sounder for cloud-free conditions. The required data, therefore, may be entirely obtained from the DMSP/SSH sensors. The procedure applies only for cloud-free conditions, hence the presence of clouds must be sensed. Since sea surface temperature measurements can only be made under cloud-free conditions, this restriction on the retrieval of water vapor information is not critical.

5. CONCLUSIONS

The 220 simulated radiances sets were used to estimate the coefficients of a $\underline{\underline{D}}$ matrix linear operator for use in estimating precipitable water using infrared radiance and temperature level data. The residual errors expected using the statistical regression procedure are less than 20 percent of the mean values for precipitable water in the lower levels of the atmosphere. Smith and Woolf (1976) report better results for Nimbus-6 data when the infrared and microwave data are combined. The microwave channels are relatively transparent and water vapor may be sensed to the surface. The weighting functions displayed in Figures 5 and 6 show that under warm, humid conditions, water vapor near the surface cannot be sensed by the DMSP/SSH sounder. The success of the combined sounding plus temperature profile algorithm for warm, humid profiles is a result of the natural correlation between temperature and water vapor. Improved water vapor retrievals could be obtained if additional infrared sounding channels were provided in a less opaque region of the water vapor spectrum. A number of the current F-channels on the SSH package are redundant and may be eliminated without loss in sensor capability.

The Statistical Parameter Estimation Procedure was used for water vapor retrievals. It can also be successfully used for the extraction of temperature profile data from the CO_2 sounder channels. The National Oceanic and Atmospheric Administration (NOAA) operational procedures are now being changed to use the statistical parameter estimation procedure for profile estimation (Smith and Woolf, 1976). A similar move for the extraction of data from the DMSP/SSH data is recommended. The simultaneous inversion of E, F and Z channel data to estimate both temperature and water vapor parameters has the advantage of automatically incorporating the temperature level information for the extraction of water vapor data as proposed in this report, plus automatically providing the water vapor corrections for the temperature sounder channels.

REFERENCES

1. McClatchey, R. A., W. S. Benedict, A. S. Clough, D. E. Burch, R. F. Calfee, K. Fox, L. S. Rothman and J. S. Garing, 1973: AFCRL Atmospheric Absorption Line Parameters Compilation. AFCRL-TR-73-0096, Air Force Cambridge Research Laboratory.

2. Wachtmann, R. F., March, 1975: "Expansion of Atmospheric Temperature - Moisture Profiles in Empirical Orthogonal Functions for Remote Sensing Applications", Presented Spring Conf. Optical Society of America.

3. *Gaut, N. E., E. C. Reifenstein III and D. Chang, 1972:* Microwave Properties of the Atmosphere, Clouds and the Oceans. Final Report NAS 5-21624, Environmental Research & Technology, Inc. Concord, Massachusetts.

4. Chandrasekhar, S., 1960: Radiative Transfer, Dover Publications.

5. Burch, D. E., D. A. Gryvnak and F. J. Gates, 1974: Continuum Absorption by H_2O Between 330 cm^{-1} and 825 cm^{-1}, AFCRL-TR-74-0377, Air Force Cambridge Research Laboratory.

6. Smith, W. L., and H. B. Howell, 1971: "Vertical Distributions of Atmospheric Water Vapor from Satellite Infrared Spectrometer Measurements", J. Appl. Meteorol. 10, 1026-1034.

7. Smith, W. L., and H. M. Woolf, 1976: "The Use of Eigenvectors of Statistical Covariance Matrices for Interpreting Satellite Sounding Radiometer Observations", J. Atmosph. Sci. 23, 1127-1140.

8. Lorentz, E. N., 1956: Empirical Orthogonal Functions and Statistical Weather Prediction. Statistical Forecasting Project Scientific Report No. 1, Massachusetts Institute of Technology.

9. Barnes Engineering Co., 1975: Spectral Digitization Data for System and Bandpass Filters of SSH Flight I, S/N 002. Continued F04701-73-C-0036.

10. Goody, R. M., 1964: Atmospheric Radiation, Oxford.

11. Hanel, R. A., and B. J. Conrath, 1970: "Thermal Emission Spectra of the Earth and Atmosphere from the NIMBUS 4 Michelson Interferometer Experiment", Nature 328, 143.

12. Cogan, J. L., and J. H. Willand, 1975: Mapping of Sea Surface Temperature by the DMSP Satellite, Environmental Research & Technology, Inc.

13. Shen, W. C., and W. L. Smith, 1972: Statistical Estimation of Precipitable Water with SIRS-B Water Vapor Radiation Measurements. Preprint Conf. on Atmos. Radiation, American Meteorol. Soc. Boston, 145-151.

APPENDIX A

SOFTWARE DESCRIPTION

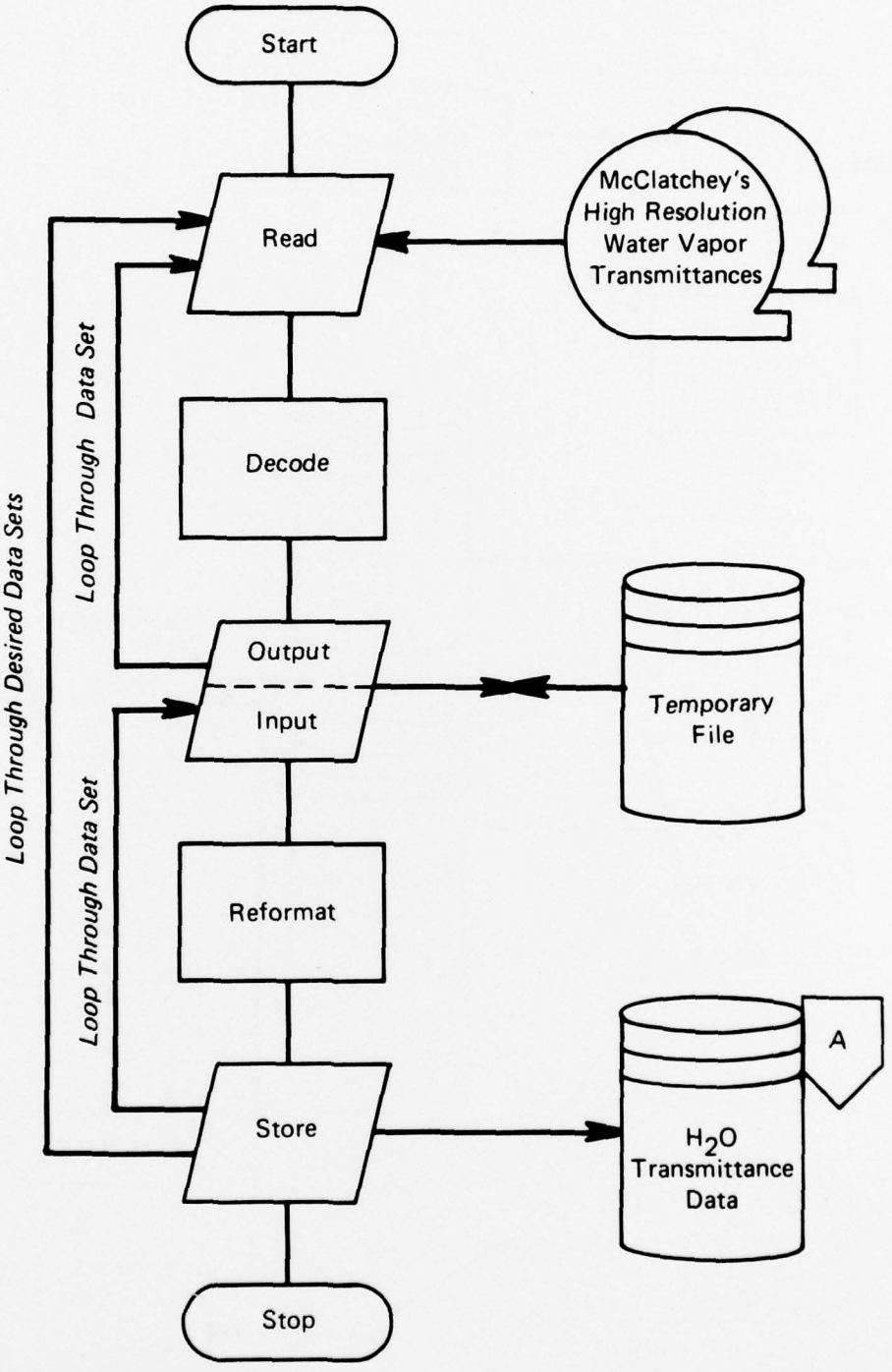

Figure A-1 Initial Transmittance Processing

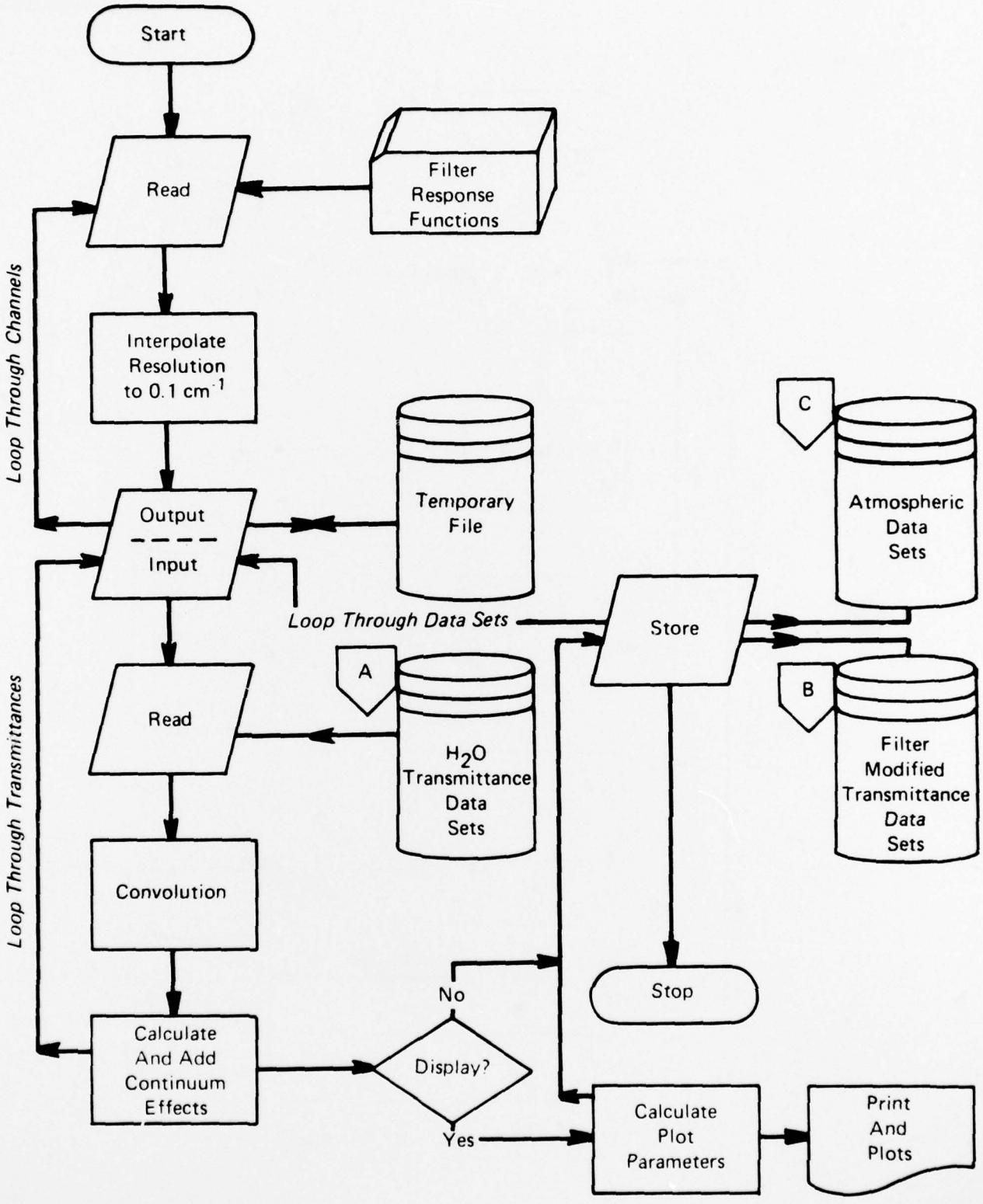

Figure A-2 Filter Modified Transmittance Data Set Generation Scheme

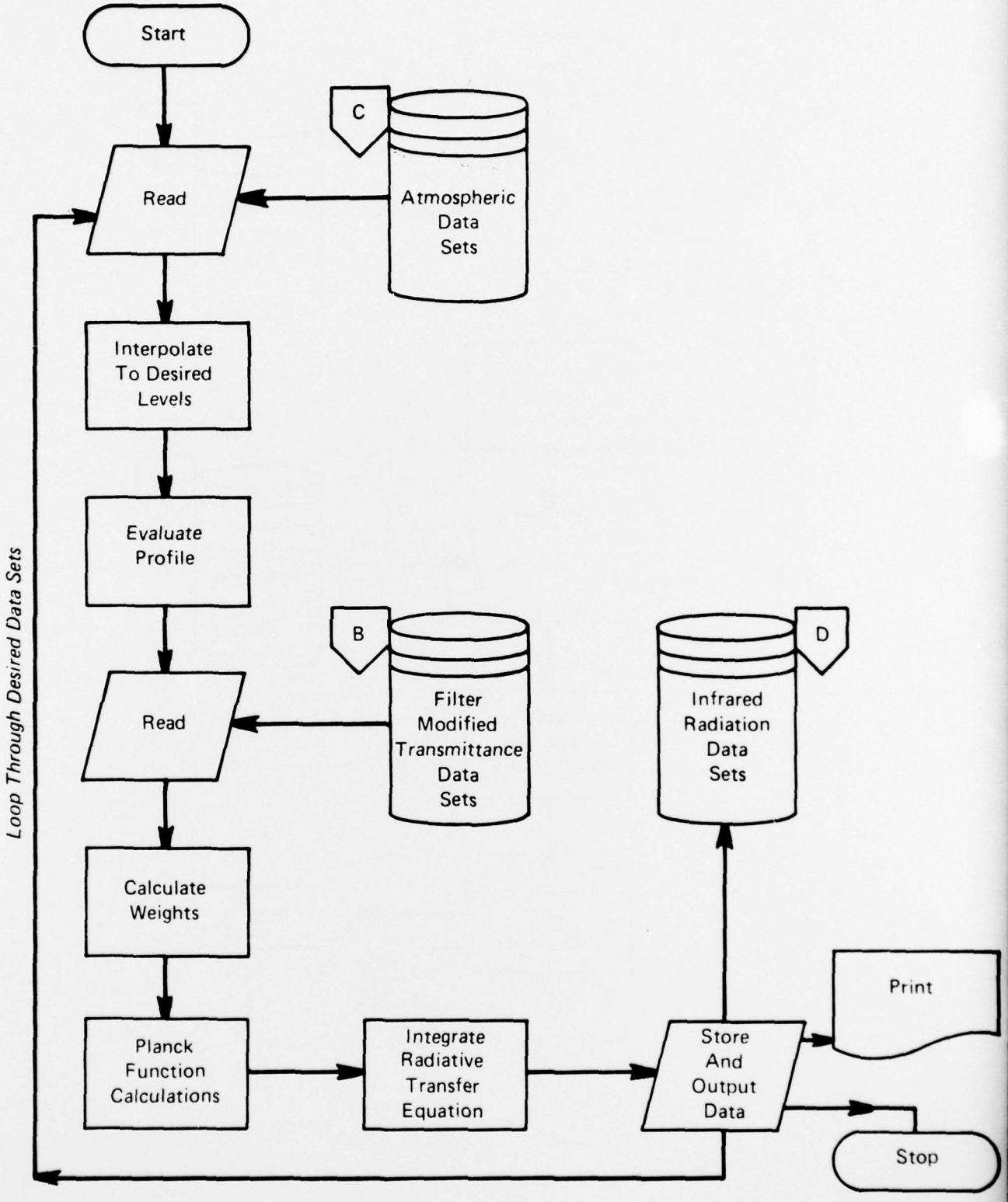

Figure A-3 Simulated Radiance Calculations

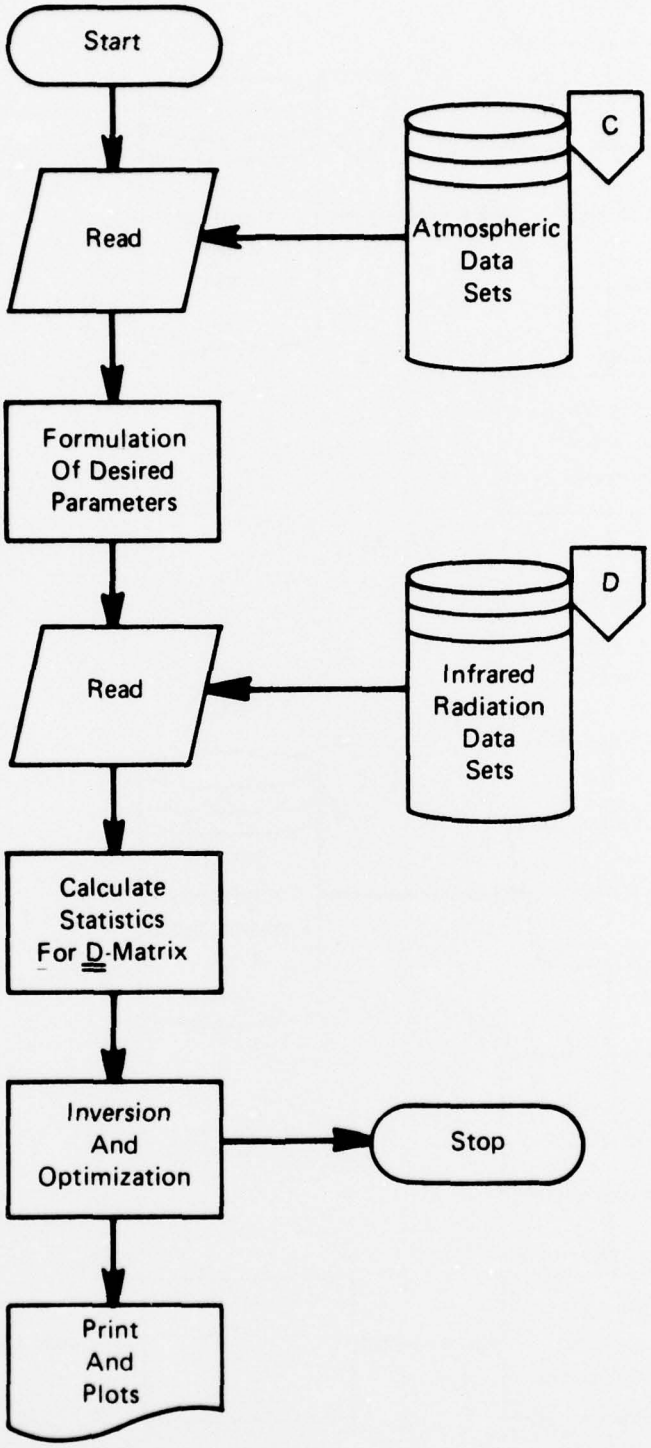

Figure A-4 Retrieval and Optimization

APPENDIX B

$\underline{\underline{D}}$ MATRICES

D MATRICES

DATA		PARAMETERS												
W(P)	Avg.	IR1	IR2	IR3	IR4	IR5	IR6	IR7	IR8	T(1000)	T(920)	T(850)	T(700)	T(500)
Channels 1-8 and 5 Temperature Levels														
W(1000)	2.86	4.987	3.147	1.176	0.141	-8.349	-4.101	-6.650	-9.298	12.661	13.436	14.187	12.705	16.513
W(920)	1.97	3.821	2.447	0.998	0.103	-6.725	-3.305	-5.411	-8.309	7.508	9.291	11.017	11.416	14.630
W(850)	1.46	2.947	1.929	0.894	0.140	-5.379	-2.617	-4.354	-7.561	5.142	7.044	8.885	9.824	12.604
W(700)	0.66	1.280	0.851	0.459	0.033	-2.812	-1.381	-2.303	-4.600	1.670	3.237	4.753	5.986	7.621
W(500)	0.14	0.049	-0.009	-0.052	-0.139	-0.630	-0.382	-0.526	-7.243	0.045	0.570	1.079	1.583	1.916
Channels 1-8 and 4 Temperature Levels														
W(1000)	2.86	4.991	2.974	1.056	0.296	-8.291	-3.796	-5.976	-10.037	11.044	15.885	20.572	21.021	
W(920)	1.97	3.786	2.261	0.900	0.285	-6.606	-2.954	-4.699	-9.433	5.418	11.436	17.262	19.771	
W(850)	1.46	2.909	1.757	0.807	0.309	-5.255	-2.284	-3.700	-8.676	3.132	8.886	14.456	17.323	
W(700)	0.66	1.261	0.741	0.395	0.137	-2.724	-1.171	-1.884	-5.344	3.517	4.350	8.221	10.646	
W(500)	0.14	0.051	-0.035	-0.075	-0.118	-0.612	-0.335	-0.426	-0.876	-0.239	0.854	1.912	2.671	
Channels 1-7 and 5 Temperature Levels														
W(1000)	2.86	7.796	4.433	0.150	-1.073	-11.760	-6.479	-9.444		9.468	11.214	12.908	12.782	14.815
W(920)	1.97	6.226	3.567	0.173	-0.912	-9.773	-5.402	-7.960		4.724	7.310	9.816	11.352	13.199
W(850)	1.46	5.102	2.937	0.171	-0.763	-8.151	-4.510	-6.686		2.632	5.244	7.775	9.722	11.323
W(700)	0.66	2.566	1.456	0.040	-0.501	-4.497	-2.529	-3.734		0.161	2.143	4.063	5.891	6.859
W(500)	0.14	0.249	0.086	-0.116	-0.223	-0.896	-0.563	-0.752		-0.190	0.398	0.967	1.565	1.798
Channels 4, 5, 7 and 8 and 5 Temperature Levels														
W(1000)	2.86				8.856	-9.610		-6.449	-13.379	14.561	14.538	14.518	12.012	16.360
W(920)	1.97				6.720	-7.607		-5.201	-11.586	8.986	10.155	11.288	10.893	14.547
W(850)	1.47				5.494	-6.197		-4.262	-10.002	6.230	7.684	9.093	9.447	12.533
W(700)	0.66				2.435	-3.350		-2.398	-5.552	2.073	3.481	4.844	5.857	7.581
W(500)	0.14				-0.292	-0.761		-0.659	-0.703	2.390	0.563	1.085	1.596	1.908
Channel 8 and 5 Temperature Levels														
W(1000)	2.86								-21.269	15.449	15.746	16.035	11.972	15.783
W(920)	1.97								-18.164	9.808	11.203	12.203	10.862	14.118
W(850)	1.47								-15.438	6.956	8.583	10.158	9.419	12.175
W(700)	0.66								-8.979	2.645	4.093	5.496	5.831	7.448
W(500)	0.14								-2.124	0.348	0.836	1.304	1.578	1.981

$\underline{D}$ MATRICES (CONTINUED)

DATA		PARAMETERS												
W(P)	Avg	IR1	IR2	IR3	IR4	IR5	IR6	IR7	IR8	T(1000)	T(920)	T(800)	T(700)	T(500)
No IR Channels and 5 Temperature Levels														
W(1000)	2.86									7.056	7.010	6.965	6.445	6.561
W(920)	1.97									2.624	3.750	4.839	6.048	6.309
W(850)	1.46									0.844	2.251	3.614	5.286	5.569
W(700)	0.66									-0.916	0.414	1.701	3.392	3.630
W(500)	0.14									-0.495	-0.037	0.406	1.000	1.079
Channels 1-8 But No Temperature														
W(1000)	2.86	12.606	5.912	-2.955	-4.020	-18.177	-10.981	-12.297	35.457					
W(920)	1.97	9.450	4.427	-2.236	-3.061	-13.297	- 8.360	- 9.835	25.373					
W(850)	1.46	7.394	3.467	-1.746	-2.404	-10.852	- 6.584	- 7.792	19.232					
W(700)	0.66	3.540	1.602	-0.975	-1.305	- 5.487	- 3.381	- 3.990	9.270					
W(500)	0.14	0.512	0.134	-0.365	-0.407	- 1.176	- 0.794	- 0.858	2.246					
Channels 1-7 But No Temperature														
W(1000)	2.86	-3.076	-1.645	2.626	0.873	5.341	3.355	5.251						
W(920)	1.97	-1.818	-0.988	0.119	0.472	3.065	1.911	3.010						
W(850)	1.46	-1.172	-0.642	0.065	0.290	1.946	1.209	1.910						
W(700)	0.66	-0.604	-0.383	-0.089	0.002	0.693	0.380	0.669						
W(500)	0.14	-0.484	-0.347	-0.166	-0.113	0.315	0.116	0.292						
Channels 4, 5, 7 & 8 But no Temperature														
W(1000)	2.86				25.182	-36.356		-22.702	38.692					
W(920)	1.97				18.645	-27.351		-17.235	27.732					
W(850)	1.46				14.506	-21.406		-13.555	21.038					
W(700)	0.66				6.347	-10.452		- 6.755	10.073					
W(500)	0.14				0.127	- 0.187		- 1.331	2.345					

$\underline{\underline{D}}$ MATRICES (CONTINUED)

DATA		PARAMETERS												
W(P)	Avg	IR1	IR2	IR3	IR4	IR5	IR6	IR7	IR8	T(1000)	T(920)	T(800)	T(700)	T(500)
Channels 4, 5 & 7 But no Temperature														
W(1000)	2.86				-5.515	8.445		7.584						
W(920)	1.97				-3.370	4.882		4.365						
W(850)	1.46				-2.201	3.111		2.775						
W(700)	0.66				-1.654	1.286		1.065						
W(500)	0.14				-1.732	0.781		0.567						
Channel 8 But No Temperature														
W(1000)	2.86								11.770					
W(920)	1.97								7.257					
W(850)	1.46								4.936					
W(700)	0.66								1.828					
W(500)	0.14								0.389					